

First-Order Local Invariants of Stable Maps from 3-Manifolds to \mathbb{R}^3

R. OSET SINHA & M. C. ROMERO FUSTER

1. Introduction

The study of topological invariants of stable maps has been one of the main problems in singularity theory in the last decades. An important question concerns the global study of stable maps between 3-manifolds. This is a very difficult problem when one tries to study it in a general setting. Little is known from the global viewpoint; even in the particular case of stable maps from the 3-sphere to Euclidean 3-space. In [19], Vassiliev introduced a method to define isotopy invariants for stable maps in a fairly general context that has proved to be useful in the case of knots (considered as stable maps from the circle to 3-space; see [18]). Such invariants can be seen as locally constant functions on the considered subspace of stable maps, and the method is based on analyzing the structure of the discriminant set (subset of nonstable maps) in the total space of the maps in question. Vassiliev's techniques have also been used to study other subspaces of stable maps, such as immersed closed plane curves [1; 2], stable maps between surfaces [16], stable maps from surfaces into Euclidean 3-space [7], and stable maps from 3-manifolds to the plane [20]. This method, although it does not provide all the global invariants, does lead to an important set of invariants that contain all the information on multilocal behavior of the stable maps. These invariants are, in fact, related to the properties of the branch set (image of the singular set). To combine them with the global invariants related to the topology of the singular set in the source manifold (such as the graphs introduced in [8; 9; 10] for stable maps of surfaces into the plane) is to take a first step toward a global classification in each particular case of stable maps.

In order to apply this method to the case of stable maps from a closed 3-manifold to \mathbb{R}^3 , we need to know all the codimension-1 and codimension-2 phenomena for maps between 3-manifolds (or from \mathbb{R}^3 to \mathbb{R}^3 , from a local viewpoint) as well as the bifurcation diagrams for those of codimension 2. For this we have used the classification of corank-1 germs together with the information on bifurcation diagrams contained in the papers by Goryunov [6] and Marar and Tari [13]. A sufficient list of multigerms is obtained in Section 2.2 of this paper, and some of their bifurcation diagrams are calculated in the Appendix (Section 8). In Section 3 we obtain

Received November 9, 2010. Revision received May 5, 2011.

Work of both authors partially supported by DGCYT and FEDER Grant no. BMF2009-08933.

a complete set of generators for the first-order integer invariants of Vassiliev type for stable maps from a closed 3-manifold to \mathbb{R}^3 . This set comprises four invariants:

1. I_s = number of swallowtail points;
2. I_t = number of triple points;
3. $I_{A_1A_2}$ = number of intersection points of fold surfaces with cuspidal edges;
4. I_χ = Euler characteristic of the branch set.

The geometric interpretation of these invariants is discussed in Section 4. We will see that all of them are, indeed, global invariants.

We observe that some of the first-order invariants are related to those obtained by Goryunov for stable maps of surfaces to \mathbb{R}^3 in [7]. The swallowtail points and triple points in the branch sets correspond to the cross-caps and triple points in the image sets of those maps. The existence of cuspidal edges in our case introduces a new feature that leads to the invariant $I_{A_1A_2}$. Moreover, although I_χ appears in Goryunov's case, an important difference is that, for stable maps from a closed 3-manifold to \mathbb{R}^3 , I_χ is linearly independent (as shown in Section 5). It is most interesting that the natural analogue of Goryunov's linking invariant is not a local invariant in this case. Neither is a dimension-3 analogue of the generalized Bennequin invariant defined in [16].

In Section 6 we introduce some other global invariants, such as the number of connected components of the singular set and the number of cuspidal edges, that are independent of the four just listed. In fact, obtaining them requires refining some of the 1-dimensional strata in order to distinguish between those that connect or those that disconnect the singular set (or the cuspidal edges) from a global point of view.

In Section 7 we discuss the particular case of fold maps, and in Section 8 we give the proofs of the lemmas needed for Theorem 3.2.

ACKNOWLEDGMENTS. The authors would like to thank V. Goryunov and R. Wik-Atique for many valuable comments about the mathematics as well as D. Davis for his help improving the English in the article.

2. Singularities of Maps from 3-Manifolds to \mathbb{R}^3

We begin by recalling some basic definitions and results. Two smooth maps f and g from a 3-manifold M to 3-space are called *\mathcal{A} -equivalent* if there exist diffeomorphisms l and k such that $l \circ f = g \circ k$. A smooth map f is said to be *stable* if all maps sufficiently close to f (in the Whitney C^∞ -topology) are \mathcal{A} -equivalent to f . The critical set Σ_f of a stable map f consists of disjoint embedded (critical) surfaces. Each surface consists of fold points together with curves of cusp points (i.e., points whose image is a cusp point of the branch set $f(\Sigma_f)$) along which there may be isolated swallowtail points. The following are normal forms for the germs of f at these critical points (see [5]):

- (a) $f(x, y, z) = (x, y, z^2)$, fold point;
- (b) $f(x, y, z) = (x, y, z^3 + xz)$, cusp point;
- (c) $f(x, y, z) = (x, y, z^4 + xz + yz^2)$, swallowtail point.

The branch set of a stable map may also have self-intersections as follows:

- (d) transversal crossings of fold surfaces (along regular curves);
- (e) transversal intersection of a cuspidal edge with a fold surface (at isolated points);
- (f) isolated triple points formed by the intersection of three fold surfaces in general position.

Figure 1 illustrates (a)–(f) for the local geometry of the branch set of a stable map.

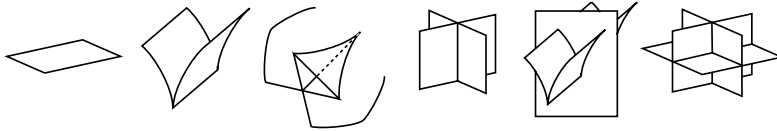


Figure 1 Branch sets of stable maps from \mathbb{R}^3 to \mathbb{R}^3

If f and g are \mathcal{A} -equivalent then there is a diffeomorphism of the manifold carrying the critical set of f to the critical set of g , and similarly for the branch sets of f and g . Clearly, any diffeomorphism invariant of the critical set or of the branch set will be an \mathcal{A} -invariant of f . The number of connected components of the singular set and the topological type of its complement are invariants.

Table 1, which is based on [6] and [13], lists normal forms for simple corank-1 monogermers of maps from \mathbb{R}^3 to \mathbb{R}^3 and includes all the \mathcal{A} -classes of codimension 0 through codimension 5. Here the $P(x, y)$ are polynomials in two variables and $\mu(P)$ denotes the Milnor number of P . Let $\mathcal{O}_{n,p}$ be the ring of smooth germs $(\mathbb{R}^n, 0) \rightarrow (\mathbb{R}^p, 0)$; then, given $f \in \mathcal{O}_{n,p}$, the \mathcal{A}_e -codimension of f is equal to $\dim_{\mathbb{R}} \frac{\mathcal{O}_{n,p}}{\mathcal{T}\mathcal{A}_e \cdot f}$, where $\mathcal{T}\mathcal{A}_e \cdot f = \{ \sum_{i=1}^n \frac{\partial f}{\partial x_i} g_i \mid g = (g_1, \dots, g_n) \in \mathcal{O}_{n,n} \} + \{ h \circ f \mid h \in \mathcal{O}_{p,p} \}$. We observe that, for $n = p = 3$, the \mathcal{A} -codimension of the germ in each case is the \mathcal{A}_e -codimension + 3 *except* for the stable germs: the fold, the cusp, and the swallowtail all have \mathcal{A}_e -codimension 0 but have \mathcal{A} -codimension 1, 2, and 3 (respectively). We also observe that the \mathcal{A}_e -codimension coincides with the codimension of the stratum of nonstable maps in $C^\infty(M, \mathbb{R}^3)$ to which the germ belongs as a map.

Table 1

Name	Normal form	\mathcal{A}_e -codimension
A_1	(x, y, z^2)	0
$3_{\mu(P)}$	$(x, y, z^3 + P(x, y)z)$	$\mu(P)$
4_1^k	$(x, y, z^4 + xz \pm y^k z^2), k \geq 1$	$k - 1$
4_2^k	$(x, y, z^4 + (y^2 \pm x^k)z + xz^2), k \geq 2$	k
5_1	$(x, y, z^5 + xz + yz^2)$	1
5_2	$(x, y, z^5 + xz + y^2 z^2 + yz^3)$	2

2.1. Monogermers of Codimension 1 and 2

According to Table 1, the corank-1 monogermers of \mathcal{A}_e -codimension 1 are given as follows.

- (i) Germs of type 3_1 . This includes three different classes corresponding to $P(x, y) = x^2 + y^2$, $P(x, y) = x^2 - y^2$, and $P(x, y) = -x^2 - y^2$; we denote them (respectively) as 3_1^{++} , 3_1^{+-} , and 3_1^{--} .
- (ii) Germs of type 4_1^2 . Here there are two different classes corresponding to signs + or - in the normal form; these are denoted by 4_1^{2+} and 4_1^{2-} , respectively.
- (iii) The germ 5_1 .

Figure 2 shows the transitions in the branch set $f(\Sigma_f)$ for all the codimension-1 germs just listed.

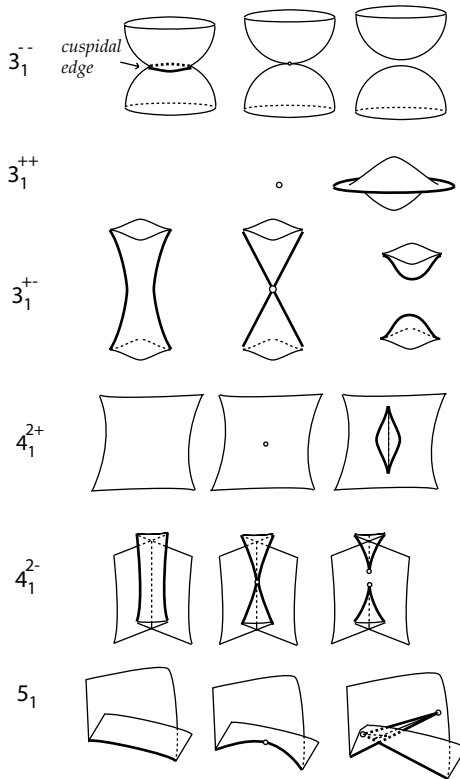


Figure 2 Codimension-1 transitions for germs

The corank-1 monogermers lying in the codimension-2 stratum are the following.

- (i) Germs of type 3_2 . This includes two different classes corresponding to $P(x, y) = x^2 \pm y^3$ and $P(x, y) = -x^2 \pm y^3$, which we denote by 3_2^+ and 3_2^- (respectively).
- (ii) The germ 4_1^3 .

- (iii) Germs of type 4_2^2 . This includes two different classes corresponding to the signs + or – in the normal form; they are denoted by 4_2^{2+} and 4_2^{2-} , respectively.
- (iv) The germ 5_2 .
- (v) The nonsimple germ 6_1 , whose normal form is $(x, y, z^6 + yz^2 + xz)$ (see [6]).

The corank-2 germs of \mathcal{A}_e -codimension 1 are the hyperbolic and elliptic umbilics, U^h and U^e (purse and pyramid, as in [3]), whose normal forms are:

$$(x, yz, y^2 \pm z^2 + xy).$$

The corank-2 germs of \mathcal{A}_e -codimension 2 will not be needed for reasons that are given later.

2.2. Multigerms of Codimension 1 and 2

Most of the normal forms of the multigerms can be obtained by augmentations, monic and binary concatenations, or a third operation (which merges the two previous ones) of known classifications (see [4]). This does not yield a complete list, however, and those that cannot be obtained in this way are known as *primitive*. In order to find out what primitive multigerms may exist, we propose a geometrical method based on the contact between the different branches. We then propose a normal form (which, it can be proved, is of adequate codimension; since the bifurcation diagrams are topologically different from the other ones, they must belong to different \mathcal{A} -classes).

We shall see later on that, in order to determine the first-order invariants of Vasiliev type for stable maps from closed 3-manifolds to \mathbb{R}^3 , it is *not* necessary to analyze the bifurcation sets of corank-2 multigerms (or monogerms). So in this paper we study only corank-1 multigerms, which involve only A_k singularities and for which it is known that their corresponding orbits in the multijet space are defined by submersions in the stable case and by isolated complete intersection singularities (ICIS) in the finitely determined case [6].

A multigerm can be viewed as a coupling of different germs $f_i: (\mathbb{R}^3, x_i) \rightarrow (\mathbb{R}^3, y)$ with the x_i all different and with the same image $y \in \mathbb{R}^3$. In order to determine their codimension, we distinguish between the following phenomena.

- (i) Simple conjunction of germs: there is no branch-to-branch tangency in the critical value set.
- (ii) Tangential conjunction of Morse type: at least two of the branches of the critical value set have Morse-type contact.
- (iii) Degenerate tangential conjunction: at least two of the branches of the critical value set have degenerate contact.

Here we understand “contact” in the sense of Montaldi’s work [14]. We thus associate a contact function to each pair of tangent strata (surfaces or curves, in our case) whose singularities describe the contact type. Then we say that a contact between two strata (submanifolds) is nondegenerate (of Morse type) or degenerate according as whether the corresponding contact function is of Morse type or not.

Denote by $C(i_1, \dots, i_r)$, $C_T(i_1, \dots, i_r)$, and $C_{DT}(i_1, \dots, i_r)$ the \mathcal{A} -codimensions of the simple, tangential, and degenerate tangential conjunctions of r germs with respective \mathcal{A} -codimensions i_1, \dots, i_r . We then have the following criteria:

- (i) $C(i_1, \dots, i_r) = i_1 + \dots + i_r$;
- (ii) $C_T(i_1, \dots, i_r) \geq i_1 + \dots + i_r + r_t$, where we suppose that each tangency affects just two branches and r_t depends on the number and type of tangencies;
- (iii) $C_{DT}(i_1, \dots, i_r) \geq i_1 + \dots + i_r + r_t + r_d$, where we suppose that each tangency affects just two branches, r_t is as before, and r_d depends on the number and type of degenerate tangencies.

To justify these criteria, we use the following result. Consider $S = \{x_1, \dots, x_r\} \subset \mathbb{R}^n$, $y \in \mathbb{R}^p$, and $f : (\mathbb{R}^n, S) \rightarrow (\mathbb{R}^p, y)$ a nonstable multigerms of \mathcal{A} -codimension s , where $s > n$ (since otherwise it would be stable). Assume that f is both k -determined and \mathcal{A} -simple. Suppose there exists a smooth submanifold $X \subset {}_rJ^k(\mathbb{R}^n, \mathbb{R}^p)$ such that, for all $g : \mathbb{R}^n \rightarrow \mathbb{R}^p$ and all $\{z_1, \dots, z_r\} \subset \mathbb{R}^n$, we have that ${}_rJ^k g(z_1, \dots, z_r) \in X$ if and only if the multigerms of g in $\{z_1, \dots, z_r\}$ is \mathcal{A} -equivalent to f .

LEMMA 2.1. $\text{cod}_{{}_rJ^k(\mathbb{R}^n, \mathbb{R}^p)} X = s + (r - 1)p$.

Proof. This is proved by standard multijet and transversality techniques; for a detailed account, see [17]. □

If the codimensions of the monogermers involved are i_1, \dots, i_r , then each one defines a smooth submanifold in the appropriate jet space of respective codimensions i_1, \dots, i_r . These submanifolds are defined (respectively) by i_1, \dots, i_r equations.

If we consider the submanifold $X \subset {}_rJ^k(\mathbb{R}^n, \mathbb{R}^p)$ defined by the equations that define the multigerms—in other words, the equations that define each of the germs involved (which are independent because they involve different variables) plus the equations that arise from all the points having the same image in the target space—then we have that the codimension of X is $i_1 + \dots + i_r + (r - 1)p$ (the $(r - 1)p$ extra equations come from $f(x_1) = \dots = f(x_r)$). From Lemma 2.1 it follows that the codimension of such a submanifold is $s + (r - 1)p$, so we deduce that the \mathcal{A} -codimension of the multigerms is $s = i_1 + \dots + i_r$.

In the case of a Morse-type tangential conjunction, the same situation is obtained but now there are extra equations arising from the tangency. One need only make sure that these new equations are independent from the rest (i.e., that the rank of the system of equations is equal to the number of equations) in order for the codimension of the submanifold X to be equal to the number of equations.

Observe that for a map $f : \mathbb{R}^3 \rightarrow \mathbb{R}^3$ the tangencies (degenerate, or otherwise) to be considered will involve either two surfaces, a surface and a curve, or two curves. According to Montaldi [14], in the case of either two surfaces or two curves, the contact is measured by a function $\phi : \mathbb{R}^2 \rightarrow \mathbb{R}$ and hence a Morse tangential contact is determined by two conditions on the 1-jet of ϕ . In the case of a surface and a curve, we have a contact function $\phi : \mathbb{R} \rightarrow \mathbb{R}$ and so a Morse tangential contact requires one condition on the 1-jet of ϕ at the contact point. In order to ensure a degenerate contact we need, in each case, for the determinant of the Hessian matrix of ϕ to vanish. This requirement imposes at least one more condition on the 2-jet—and exactly one in the case where ϕ has a singularity of \mathcal{A} -codimension 1 (i.e., a fold). We call this a *first-order degenerate tangency*. Clearly, these conditions on the derivatives of ϕ can be written as conditions on an

appropriate k -jet of the map f . Hence more precision is possible and, for a tangential conjunction of r germs with \mathcal{A} -codimensions i_1, \dots, i_r , we have the following statements.

- (ii)(a) If there is a unique Morse tangency between two fold surfaces in the branch set, then $C_T(i_1, \dots, i_r) = i_1 + \dots + i_r + 2$.
- (ii)(b) If there is a unique Morse tangency between two cuspidal edges or between two double fold curves in the branch set, then $C_T(i_1, \dots, i_r) = i_1 + \dots + i_r + 2$.
- (ii)(c) If there is a unique Morse tangency between a fold surface and either a cuspidal edge or a double fold curve in the branch set, then $C_T(i_1, \dots, i_r) = i_1 + \dots + i_r + 1$.

In the case of a first-order degenerate tangency, we simply add 1 to each of the preceding sums. Up to \mathcal{A} -codimension 5 there exist only first-order degenerate tangencies.

We shall employ the following notation for multigerms. Starting from stable germs, we use A_1 (fold), A_2 (cusps), and A_3 (swallowtails); we denote by $A_i A_j$ the simple conjunction of A_i and A_j and by A_i^k the simple conjunction of k germs of type A_i (this is the standard Arnold notation). The tangential conjunctions are indicated by the character T . For example, we denote by T_{ij} a nondegenerate tangency between the strata of singularities A_i and A_j in the branch set and by $T_{A_i A_j^k}$ a nondegenerate tangency between the strata of points A_i and A_j^k in the branch set, and so forth. We use DT to signify degenerate tangencies. Accordingly, $A_1 3_1^{+-}$ denotes a conjunction of a fold with a germ of type 3_1^{+-} ; $A_1 T_{A_1 A_1^2}$ is a quadrigerm determined by a conjunction of a fold (A_1) with the trigerms $T_{A_1 A_1^2}$, which in turn is given by a nondegenerate tangential conjunction of a fold surface and a double fold curve; DT_{11} is a degenerate tangency between two fold surfaces; and $DT_{A_1 A_1^2}$ is a degenerate tangency between a fold surface and a double fold curve.

As a consequence of these considerations, and taking into account that in our case the \mathcal{A} -codimension of a nonstable germ is given by the \mathcal{A}_e -codimension + 3, we obtain a list of multigerms that are of \mathcal{A}_e -codimension 1 and 2.

EXAMPLE 2.2. To find \mathcal{A}_e -codimension-1 bigerms (i.e., \mathcal{A} -codimension 4), we proceed as follows. Let i_1 and i_2 be the codimensions of the two monogerms involved. From criterion (i) we have $i_1 + i_2 = 4$, which implies that either $i_1 = 1$ and $i_2 = 3$ ($A_1 A_3$) or $i_1 = i_2 = 2$ (A_2^2). From criterion (ii) we have $i_1 + i_2 + r_i = 4$, which implies that either $i_1 = i_2 = 1$ and $r_i = 2$ (T_{11}) or $i_1 = 1, i_2 = 2$, and $r_i = 1$ (T_{12}). There are no possibilities for criterion (iii).

Codimension-1 Multigerms.

(i) *Bigerms.*

- 1. A_2^2 (simple conjunction of two cuspidal edges):

$$\begin{cases} (x, y, z^3 + xz), \\ (y, z^3 \pm yz, x). \end{cases}$$

2. A_1A_3 (simple conjunction of a swallowtail with a fold surface):

$$\begin{cases} (x, y, z^4 + xz^2 + yz), \\ (x^2, y, z). \end{cases}$$

3. T_{11} (tangency between two fold surfaces):

$$\begin{cases} (x, y, z^2), \\ (x, y, z^2 + y^2 \pm x^2). \end{cases}$$

These can be of two different types:

- (a) T_{11}^e (elliptic tangency with +);
 (b) T_{11}^h (hyperbolic tangency with -).
 4. T_{12} (tangency between a fold surface and a cuspidal edge):

$$\begin{cases} (x, y, z^3 + yz), \\ (x, \pm x^2 + y^2, z). \end{cases}$$

These can be of two different types:

- (a) T_{12}^l (lips-type transition with +; see Figure 3);
 (b) T_{12}^b (beaks-type transition with -; see Figure 3).

(ii) *Trigerms*.

1. $T_{A_1A_1^2}$ (tangency between a fold surface and a double fold curve; although all A_1 strata have “equal rights”, the notation emphasizes that the tangency is between a surface and a curve):

$$\begin{cases} (x, y, z^2), \\ (x, y, z^2 + y), \\ (x, y^2 + x^2, z). \end{cases}$$

2. $A_1^2A_2$ (simple conjunction of a cuspidal edge and a double fold curve):

$$\begin{cases} (x, y, z^3 + yz), \\ (x, x + y^2, z), \\ (x^2, y, z). \end{cases}$$

(iii) *Quadrigerms*. A_1^4 (simple conjunction of four fold surfaces):

$$\begin{cases} (x, y, z^2), \\ (x, y, z^2 + y), \\ (x, y^2 + x, z), \\ (x^2, y, z). \end{cases}$$

This classification is complete (see [4]). Figure 3 illustrates the codimension-1 transitions corresponding to corank-1 phenomena. For simplicity, some of the transitions are represented by the stable situations occurring in both sides of the considered codimension-1 stratum.

There are no corank-2 multigerms of codimension 1.

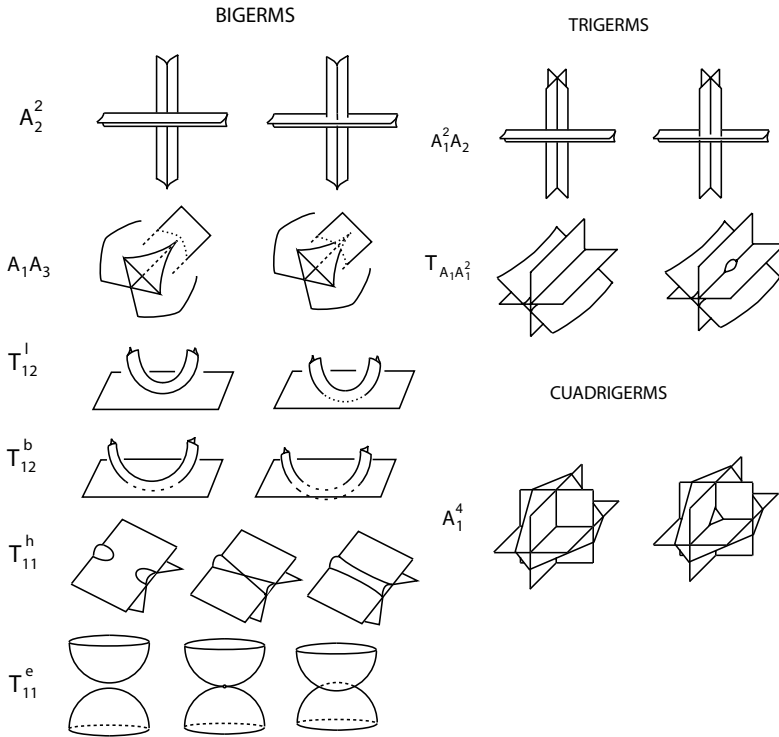


Figure 3 Codimension-1 transitions for multigerms

Codimension-2 Multigerms. For the sake of brevity, only the normal forms (together with their versal deformations) of the codimension-2 multigerms that are used will be given (see the Appendix).

(i) *Bigerms.*

1. A_13_1 (simple conjunction of a fold surface with a 3_1 germ):
 - (a) $A_13_1^{++}$;
 - (b) $A_13_1^{+-}$;
 - (c) $A_13_1^{--}$.
2. $A_14_1^2$ (simple conjunction of a fold surface with a 4_1^2 germ):
 - (a) $A_14_1^{2+}$;
 - (b) $A_14_1^{2-}$.
3. A_15_1 (simple conjunction of a fold surface with a 5_1 germ).
4. A_2A_3 (conjunction of a cusp and a swallowtail).
5. T_{13} (tangency between a fold surface and the limiting tangent vector of both the cuspidal edges and the double fold curve of the swallowtail).
6. T_{22}^1 (degeneration of A_2^2 ; the tangent vector to one of the cuspidal edges is contained in the tangent plane in the limit of the other cuspidal edge—not T_{22} , because the tangency is not between the two cuspidal edges, which would be codimension 3).

7. T_{12}^1 (a degeneration of A_1A_2 ; the tangency is between the tangent plane of the surface and the tangent plane in the limit at the cuspidal edge).
8. DT_{11} (degenerate tangential conjunction of two fold surfaces).
9. DT_{12} (degenerate tangential conjunction of a fold surface and a cuspidal edge).

(ii) *Trigerms*.

1. $A_1A_2^2$ (simple conjunction of a fold surface and two cuspidal edges).
2. $A_1^2A_3$ (simple conjunction of two fold surfaces and a swallowtail point).
3. A_1T_{11} (tangential conjunction of three fold surfaces). According to the type of tangency of the two fold surfaces involved, we have:
 - (a) $A_1T_{11}^e$ (elliptic tangency) or
 - (b) $A_1T_{11}^h$ (hyperbolic tangency).
4. A_1T_{12} (tangential conjunction of two fold surfaces and a cuspidal edge, where the tangency involves one of the fold surfaces and the cuspidal edge). Again, we have two possible types:
 - (a) $A_1T_{12}^l$ (lips);
 - (b) $A_1T_{12}^b$ (beaks).
5. $DT_{A_1A_1^2}$ (degenerate tangential conjunction between a fold surface and a double fold curve; i.e., degenerate tangential conjunction of three fold surfaces).
6. $T_{A_1^2A_2}^1$ (degeneration of $A_1^2A_2$; the tangent vector to the double point curve is contained in the tangent plane in the limit of the cuspidal edge).

(iii) *Quadrigerms*.

1. $A_1^3A_2$ (simple conjunction of a triple fold point and a cuspidal edge).
2. $A_1T_{A_1A_1^2}$ (tangential conjunction of four fold surfaces).

(iv) *Pentagerms*. A_1^5 (simple conjunction of five fold surfaces; i.e., quintuple point).

Table 2 summarizes the germs and multigerms (up to codimension 2) obtained with the method just described. Neither the corank-2 germs and multigerms of codimension 2 nor any other possible multigerms of codimension 2 that this method fails to obtain are included, since (as we shall see) they will not be needed.

3. First-Order Local Invariants of Vassiliev Type

Let M and N be smooth manifolds with M closed (compact and without boundary), and denote by $\mathcal{E}(M, N)$ the subset of \mathcal{A} -stable maps in $C^\infty(M, N)$. Two smooth maps $f, g : M \rightarrow N$ are *stably isotopic* if there exists an isotopy $F : M \times [0, 1] \rightarrow N$ such that $F_t : M \rightarrow N$ (where $F_t(x) = F(x, t)$) is \mathcal{A} -stable for all $t \in [0, 1]$, $F_0 = f$, and $F_1 = g$. Equivalently, the maps f and g are stably isotopic if they lie in the same path component of $\mathcal{E}(M, N)$.

Given a unitary commutative ring R , an *isotopy invariant with values in R* is a locally constant function $V : \mathcal{E}(M, N) \rightarrow R$. This means that, for any pair f, g of stably isotopic maps, $V(f) = V(g)$.

Vassiliev’s technique is based on analyzing an appropriate stratification of the discriminant subset, $\Delta = C^\infty(M, N) \setminus \mathcal{E}(M, N)$. In order to apply this method, the

Table 2

Monogerms	Bigerms	Trigerms	Quadrigerms	Pentagerms
<i>Stable</i>				
A_1	A_1^2	A_1^3		
A_2	A_1A_2			
A_3				
<i>Codimension 1</i>				
$3_1^{\pm\pm}$	A_2^2	$T_{A_1A_1^2}$	A_1^4	
$4_1^{2\pm}$	A_1A_3	$A_1^2A_2$		
5_1	T_{11}^e, T_{11}^h			
U^e, U^h	T_{12}^l, T_{12}^b			
<i>Codimension 2</i>				
3_2^{\pm}	$A_13_1^{\pm\pm}$	$A_1A_2^2$	$A_1^3A_2$	A_1^5
4_1^3	$A_14_1^{2\pm}$	$A_1^2A_3$	$A_1T_{A_1A_1^2}$	
$4_2^{2\pm}$	A_15_1	$A_1T_{11}^e, A_1T_{11}^h$		
5_2	A_2A_3	$A_1T_{12}^l, A_1T_{12}^b$		
6_1	T_{13}	$DT_{A_1A_1^2}$		
	DT_{11}	$T_{A_1^2A_2}^1$		
	DT_{12}			
	T_{22}^1, T_{12}^1			

subset Δ must have codimension 1 in $C^\infty(M, N)$. Then the *first-order invariants* are defined as follows. To each codimension-1 stratum we assign a *coorientation* given by a criterion that distinguishes between positive and negative crossings of a path transverse to the stratum. Next, to each codimension-1 stratum $S \subset \Delta$ we assign a transition index ξ_S (elementary jump in [16]) whose jump is 1 whenever it crosses the stratum S in a positive sense of the coorientation and is 0 whenever it crosses any other stratum. A linear combination of indices with coefficients in R determines a *Vassiliev order-1 cocycle* provided it satisfies the following *compatibility condition*: evaluating the cocycle over a generic closed path (i.e., a closed path transverse to each of the strata of Δ) around any codimension-2 stratum, the result must be zero. All the compatibility conditions together form the *coherence system*.

The order-1 invariants are obtained by integrating the order-1 Vassiliev cocycles. In order to evaluate an invariant associated to a given Vassiliev order-1 cocycle on a given map $f \in \mathcal{E}(M, N)$, we first choose a distinguished map f_0 in the same path component of $C^\infty(M, N)$ as f and associate to it some value, say $0 \in R$. Next we consider a generic path γ joining f to f_0 , which induces a generic homotopy between f and f_0 . Then the value of the invariant over f is given by

$$V(f) := \xi_V(\gamma) + V(f_0) = \sum_i n_{S_i} \xi_{S_i}(\gamma) + V(f_0),$$

where ξ_V is the order-1 cocycle that represents the invariant V . Here $\xi_{S_i}(\gamma)$ can be viewed as the intersection index $\gamma \cap S_i$ of the path γ with the stratum S_i , and n_{S_i} can be viewed as the jump of the invariant V when crossing the stratum S_i . Clearly, the compatibility condition guarantees that the result of this procedure does not depend on the chosen generic path.

These invariants are local in the sense that their jumps are determined by the diffeomorphism type of the local deformation of the image of the map (if $\dim M < \dim N$; otherwise, of the image of the singular set) at the moment of crossing the discriminant.

We now apply this method in order to determine the first-order local integer-valued invariants of stable maps between a closed 3-manifold and \mathbb{R}^3 .

3.1. Coorientation of Codimension-1 Strata

Before coorienting the codimension-1 strata, we shall distinguish between different path components of some of the strata considered previously. In each case we must account for the local variations of pre-images of the map in the branch set. We observe that, whenever there is a cuspidal edge, the number of pre-images always increases toward the “inner side” (see Figure 4). In particular, this implies that none of the codimension-1 strata corresponding to monogerms need to be refined into substrata, because the branch set of any map in the strata contains cuspidal edges that determine the distribution of pre-images in a unique way.



Figure 4 Increasing of pre-images at a cuspidal edge

We stratify the remaining codimension-1 strata as indicated in Figure 5. In order to distinguish among substrata, we use either + or −, different Greek characters (as in the case of $A_1^2 A_2$, where we distinguish among $A_1^2 A_2^\alpha$, $A_1^2 A_2^\beta$, and $A_1^2 A_2^\gamma$), or numerical indices (as in $T_{11}^{e_j}$ with $j = 0, 1, 2$). In the last case, the superscript indicates the number of arrows pointing toward a newly created component in the complement of the branch set when going through the transition.

Once this has been done, the criteria we use to coorient the different strata depend on the variation of the number of swallowtails, triple points, or $A_1 A_2$ points or the number of connected components in the complement of the branch set (considered locally). Figure 6 shows the coorientation assigned to each codimension-1 stratum, with the long arrows pointing toward the positive direction in each case. We observe that, for the strata T_{11}^{h+} , A_2^{2+} , and $A_1^{4,2}$, the branch sets obtained before and after the transitions are locally diffeomorphic and hence are not coorientable. The same thing occurs for U^h and U^e [3], so we assign an index of 0 to each of

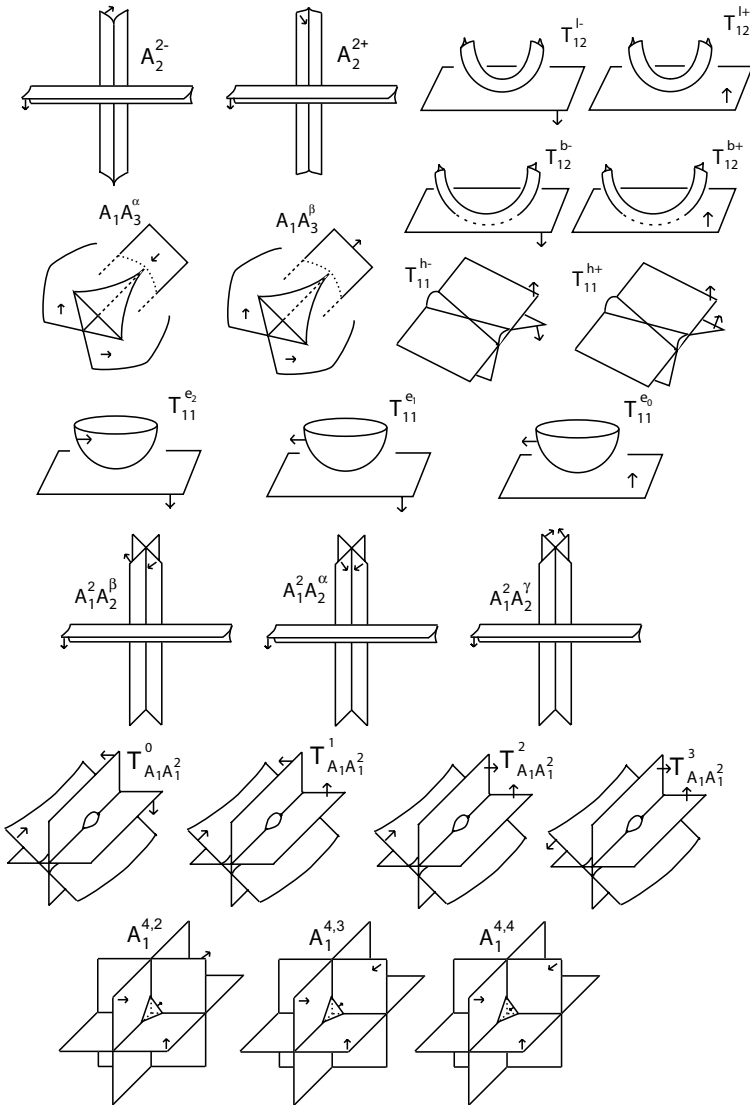


Figure 5 Substratification of codimension-1 strata

them; they are not included in Figure 6. If the work were to be done for mod 2 invariants, then the coorientations would be unnecessary and thus no strata would be assigned a zero index.

REMARK 3.1. If the orientable case were to be considered, then a distinction between positive and negative cuspidal edges would be possible according to the local degree of the map. In that case it would be possible to coorient the strata U^h and U^e ; this analysis has been done by V. Goryunov.

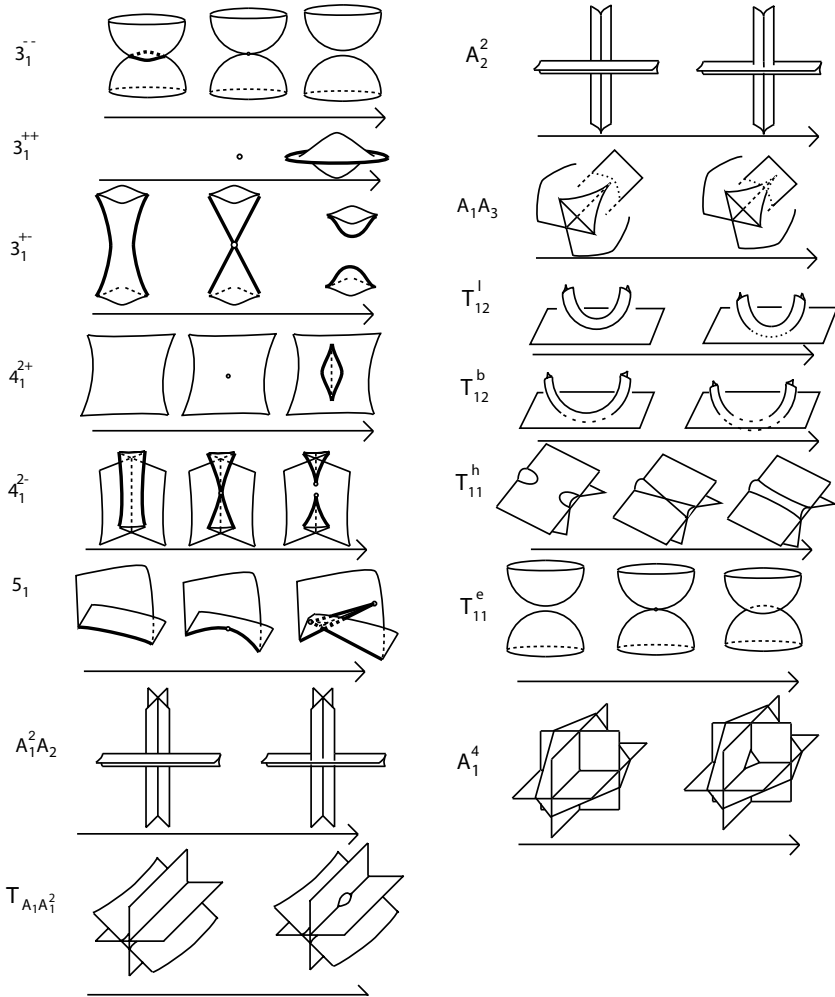


Figure 6 Cororientation of codimension-1 strata

3.2. *Compatibility Conditions and Invariants*

In this section we calculate the coherent system. For this purpose we need the bifurcation diagrams associated to a 2-parameter versal deformation of every codimension-2 phenomenon. In the case of monogerms we can use the information about bifurcation diagrams contained in [13]; to visualise the transitions in the branch sets, we use the geometric design program Superficies II [15]. The bifurcation diagrams of the multigerms are obtained by direct calculation (see [17] for details). The lemmas used to obtain the compatibility conditions are given in the Appendix.

The variation of any first-order local invariant can be seen as a linear combination of indices attached to the different codimension-1 strata. Denoting by ΔS the

transition index of S , we have that an invariant I can be expressed by a cocycle as $\Delta I = \sum n_{S_i} \Delta S_i$, where $n_{S_i} \in \mathbb{R}$ and the S_i are the codimension-1 strata.

Now the compatibility conditions (vanishing of ΔI along any closed path in $C^\infty(M, \mathbb{R}^3)$) force the existence of some relations between the different n_{S_i} , which we investigate in the Appendix lemmas. Combining all those relations, we obtain the following coherent system of equations:

- (i) $n_{3_1^{++}} = n_{3_1^{+-}} = n_{3_1^{-+}}$;
- (ii) $n_{4_1^{2+}} = n_{4_1^{2-}}$;
- (iii) $n_{A_1^2 A_2^\alpha} = n_{A_1^2 A_2^\beta} = n_{A_1^2 A_2^\gamma}$;
- (iv) $n_{A_1^{4,3}} = n_{A_1^{4,4}} = 0$;
- (v) $n_{A_1 A_3^\alpha} = n_{A_1 A_3^\beta}$;
- (vi) $n_{T_{A_1 A_1^2}^0} = n_{T_{A_1 A_1^2}^1} = n_{T_{A_1 A_1^2}^2} = n_{T_{A_1 A_1^2}^3}$;
- (vii) $n_{T_{12}^{b-}} = n_{T_{12}^{b+}} = n_{T_{12}^{l+}} = n_{T_{12}^{l-}}$;
- (viii) $n_{T_{11}^{e0}} = n_{T_{11}^{h-}} = n_{T_{11}^{e2}} = n_{T_{11}^{e1}} = 0$;
- (ix) $n_{A_1 A_3^\alpha} + n_{A_1 A_3^\beta} - n_{T_{12}^{b+}} - n_{T_{A_1 A_1^2}^1} - n_{T_{12}^{l+}} = 0$;
- (x) $n_{A_1 A_3^\alpha} + n_{A_1 A_3^\beta} - n_{A_1^2 A_2^\gamma} - n_{A_2^{2-}} = 0$;
- (xi) $n_{T_{12}^{l+}} + n_{T_{12}^{l-}} - n_{A_2^{2-}} = 0$;
- (xii) $n_{5_1} = n_{4_1^{2+}} + n_{T_{12}^{b+}}$;
- (xiii) $n_{T_{11}^{h+}} = n_{A_2^{2+}} = n_{A_1^{4,2}} = n_{U^e} = n_{U^h} = 0$ (the non-coorientable strata).

Given all these relations, we arrive at the following result.

THEOREM 3.2. *Any 1-cocycle—that is, any integer-valued function I satisfying $\Delta I = 0$ on every generic homotopically trivial closed path in $C^\infty(M, \mathbb{R}^3)$ for M a closed 3-manifold—can be written (up to an additive constant) as a linear combination of the following four generators:*

$$\begin{aligned} \Delta I_1 &= \Delta 3_1; \\ \Delta I_2 &= \Delta 4_1^2 + \Delta 5_1; \\ \Delta I_3 &= \Delta T_{12} + \Delta A_1 A_3 + 2\Delta A_2^{2-} + \Delta 5_1; \\ \Delta I_4 &= 2\Delta T_{A_1 A_1^2} + \Delta A_1 A_3 + 2\Delta A_1^2 A_2. \end{aligned}$$

Here $\Delta 3_1, \Delta 4_1^2, \Delta T_{12}, \Delta A_1 A_3, \Delta T_{A_1 A_1^2}$, and $\Delta A_1^2 A_2$ denote the sums of the indices of their corresponding substrata (e.g., $\Delta 4_1^2 = \Delta 4_1^{2+} + \Delta 4_1^{2-}$).

4. Geometrical Interpretation of the Generators

For computational purposes it is convenient to give a geometrical-topological interpretation of these invariants, which allows us to obtain the value of an invariant on a given stable map f directly from its branch set—in other words, without the need to find a generic path joining it with a distinguished map f_0 . We shall prove the following result.

THEOREM 4.1. *For M a closed 3-manifold, any first-order local invariant of $C^\infty(M, \mathbb{R}^3)$ stable maps is, modulo order-0 invariants (constants), a linear combination of the following four invariants, whose cocycles are expressed in terms of the generators.*

(i) I_s , the number of swallowtails:

$$\Delta I_s = 2\Delta I_2 = 2\Delta 4_1^2 + 2\Delta 5_1.$$

(ii) I_t , the number of triple points; its jump in terms of the transition indices is

$$\Delta I_t = \Delta I_4 = 2\Delta T_{A_1A_1^2} + \Delta A_1A_3 + 2\Delta A_1^2A_2.$$

(iii) $I_{A_1A_2}$, the number of A_1A_2 points (intersections of fold surfaces with cuspidal edges):

$$\Delta I_{A_1A_2} = 2\Delta I_3 = 2\Delta T_{12} + 2\Delta A_1A_3 + 4\Delta A_2^{2-} + 2\Delta 5_1.$$

(iv) I_χ , the Euler characteristic of the branch set:

$$\begin{aligned} \Delta I_\chi &= 2\Delta I_1 + \Delta I_2 + \Delta I_4 \\ &= 2\Delta 3_1 + \Delta 4_1^2 + \Delta 5_1 + 2\Delta T_{A_1A_1^2} + \Delta A_1A_3 + 2\Delta A_1^2A_2. \end{aligned}$$

Proof. The proof of the first three invariants is a matter of direct observation, as the strata involved in I_2 , I_4 , and I_3 are the only codimension-1 strata that create new swallowtail points (in pairs), new triple points, and new A_1A_2 points (in pairs), respectively. The proof of the fourth invariant is given next. □

4.1. The Euler Characteristic As a Vassiliev Invariant

Izumiya and Marar [12] proved that, given a stable C^∞ mapping $f : N \rightarrow P$ from a closed surface N to a 3-manifold P , the following formula holds:

$$\chi(f(N)) = \chi(N) + T(f) + \frac{C(f)}{2};$$

here $T(f)$ is the number of triple points of f and $C(f)$ is the number of cross-caps. In [11] Houston remarked that, since $T(f)$ and $C(f)$ are Vassiliev invariants in Goryunov’s case [7] and since $\chi(N)$ is constant, it follows that $\chi(f(N))$ is also a Vassiliev invariant. However, since it is a linear combination of $T(f)$ and $C(f)$, it adds no new information to Goryunov’s list.

In our case this formula may be reinterpreted as

$$\chi(\Delta) = \chi(\Sigma_f) + T(f) + \frac{S(f)}{2},$$

where Σ is the singular set, $\Delta = f(\Sigma_f)$ is the branch set, and $S(f)$ is the number of swallowtails. The difference is that here $\chi(\Sigma_f)$ is not constant; in fact, the three members of the 3_1 family change its value. Although Σ_f might be nonconnected (in which case some extra terms would be added on the right-hand side of the formula), these considerations motivate our next theorem.

THEOREM 4.2. *The Euler characteristic of the branch set, $\chi(f(\Sigma_f))$, is a Vassiliev invariant (namely, I_χ) whose cocycle in terms of the generators is given by*

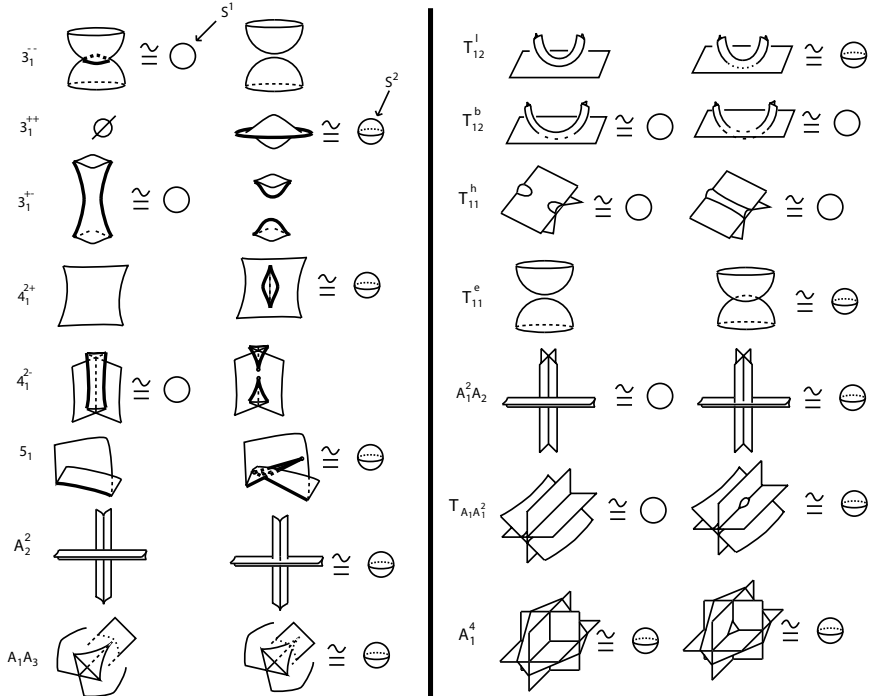


Figure 7 Homotopy equivalences of the codimension-1 strata before and after the transition

$$\begin{aligned} \Delta I_\chi &= 2\Delta I_1 + \Delta I_2 + \Delta I_4 \\ &= 2\Delta 3_1 + \Delta 4_1^2 + \Delta 5_1 + 2\Delta T_{A_1A_1^2} + \Delta A_1A_3 + 2\Delta A_1^2A_2. \end{aligned}$$

Proof. We need to check that the variation of the Euler characteristic of the branch set when crossing each codimension-1 strata is the same as the coefficient corresponding to that strata in ΔI_χ .

In fact, the calculations may be done locally (in order for it to be a Vassiliev invariant this must be so) because, for compact sets, there is additivity of the Euler characteristic $\chi(A \cup B) = \chi(A) + \chi(B) - \chi(A \cap B)$. Consider B_r , a closed ball of radius r . We can write

$$\chi(\Delta) = \chi(\Delta \cap B_r) + \chi(\Delta \setminus (\Delta \cap \text{int } B_r)) - \chi(\Delta \cap S_r^2),$$

where $S_r^2 = \partial B_r$; since $\chi(\Delta \setminus (\Delta \cap \text{int } B_r))$ and $\chi(\Delta \cap S_r^2)$ do not vary when crossing a codimension-1 strata, we need only check what happens to $\chi(\Delta \cap B_r)$.

Note that the branch set of any stabilization of a codimension-1 strata (the pictures on the left and right of the transitions) is homotopy equivalent to S^2 , S^1 , or a collection of contractible components. Given that $\chi(S^1) = 0$, $\chi(S^2) = 2$, and $\chi(D) = 1$ where D is contractible, the calculations are trivial.

Figure 7 shows all the homotopy equivalences of each stratum. Those that are not equivalent to S^1 or S^2 are a union of one or two contractible components. In

Table 3

Name	RHS	LHS	Calculation
3_1^{-}	2 pts	S^1	$2 - 0 = 2$
3_1^{++}	S^2	\emptyset	$2 - 0 = 2$
3_1^{-+}	2 pts	S^1	$2 - 0 = 2$
4_1^{2+}	S^2	1 pt	$2 - 1 = 1$
4_1^{2-}	1 pt	S^1	$1 - 0 = 1$
5_1	S^2	1 pt	$2 - 1 = 1$
A_2^2	S^2	2 pts	$2 - 2 = 0$
A_1A_3	S^2	1 pt	$2 - 1 = 1$
T_{12}^l	S^2	2 pts	$2 - 2 = 0$
T_{12}^b	S^1	S^1	$0 - 0 = 0$
T_{11}^h	S^1	S^1	$0 - 0 = 0$
T_{11}^e	S^2	2 pts	$2 - 2 = 0$
$A_1^2A_2$	S^2	S^1	$2 - 0 = 2$
$T_{A_1A_1^2}$	S^2	S^1	$2 - 0 = 2$
A_1^4	S^2	S^1	$2 - 0 = 2$

Table 3, which summarizes these equivalences, “pt” stands for point. All these variations of the Euler characteristic of the branch set are equal to the corresponding coefficients in ΔI_χ . □

5. Independence of the Four Invariants

THEOREM 5.1. *The invariants obtained in Theorem 4.1 are linearly independent.*

Proof. We use integer coefficients and write a linear combination of the four invariants as

$$aI_s + bI_t + cI_{A_1A_2} + dI_\chi = 0.$$

Then we evaluate this expression over four different examples of stable maps $f_i : S^3 \rightarrow \mathbb{R}^3, i = 2, \dots, 5$, to obtain a linear system of five equations in the variables a, b, c, d (see Figure 8). The examples are constructed starting from the basic fold map of S^3 to 3-space, where the branch set is an embedded sphere of fold points. The determinant of the matrix associated to the system is $-8 \neq 0$, so the only solution to this system is $a = b = c = d = 0$. Thus we have proved that the invariants are independent in $C^\infty(S^3, \mathbb{R}^3)$.

Now consider a stable map $f : S^3 \rightarrow \mathbb{R}^3$ and a map $g : M \rightarrow \mathbb{R}^3$ for M a closed 3-manifold. We define the connected sum $f \sharp g : S^3 \sharp M = M \rightarrow \mathbb{R}^3$ as a

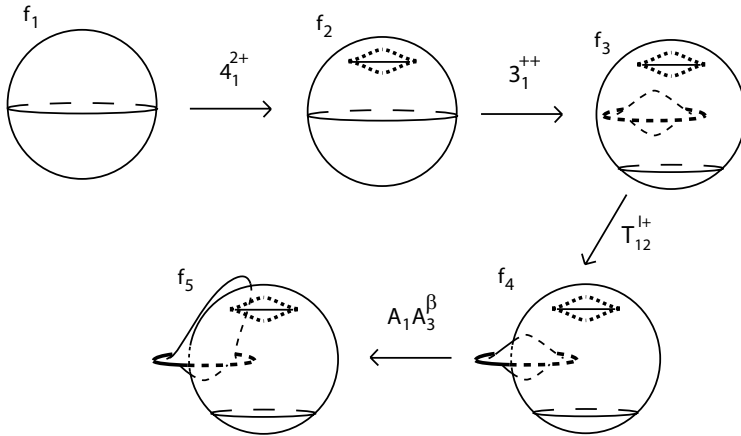


Figure 8 The branch sets of f_i and their construction

generalization of the horizontal surgery of stable maps from surfaces to the plane defined in [10] and [16]. The resulting map's branch set is the connected sum of the branch sets of f and g . This map is obtained by removing one 3-ball in S^3 and another one in M such that each contains a disk of a surface of its corresponding singular set (without cuspidal edges or double fold curves). We then join the manifolds at the removed 3-balls by an $S^2 \times I$ tube whose projection to \mathbb{R}^3 is an $S^1 \times I$ tube that does not intersect any other part of the branch sets (I is an interval). The original branch sets of f and g lie on different semispaces of \mathbb{R}^3 . It is easy to see that $I_\chi(f \sharp g) = I_\chi(f) + I_\chi(g) - 2$. We remark that I_s, I_t , and $I_{A_1 A_2}$ are additive. Evaluating the linear combination over four new examples $f_i \sharp g: M \rightarrow \mathbb{R}^3$ and taking into account the foregoing considerations, we again obtain a linear system where the determinant of the associated matrix is $12 + 6I_s(g)$, which can never be zero because $I_s(g)$ can never be negative. Hence the only solution to this system is $a = b = c = d = 0$, which proves that the invariants are independent in $C^\infty(M, \mathbb{R}^3)$ for any closed 3-manifold M . \square

The proof of Theorem 5.1 explains why the corank-2 singularities of codimension 2 are not needed and why the codimension-2 multigerms classification does not need to be complete. Any compatibility condition arising from their bifurcation diagrams would be redundant, since they would be a linear combination of the other compatibility conditions.

6. Nonlocal Invariants

If we subdivide certain codimension-1 strata (namely $3_1^{+-}, 4_1^{2-}, T_{12}^b$, and T_{11}^h) according to whether the transition does or does not affect the number of connected components of the cuspidal edges and self-intersection curves, then we can obtain additional nonlocal invariants. The name of any of the four codimension-1 strata

just mentioned, when followed by the letter a , stands for the subcase in which the curves on the left-hand side of the transition belong to two different curve components (after the transition, they become a single component); names followed by the letter b stand for the other subcases. The invariants are

$$\Delta I_6 = \Delta 3_1^{++} - \Delta 3_1^{--} + \Delta 3_1^{+-} b - \Delta 3_1^{+-} a + \Delta 4_1^{2+} + \Delta 4_1^{2-} b - \Delta 4_1^{2-} a$$

and

$$\begin{aligned} \Delta I_7 = & \Delta T_{11}^e + \Delta T_{12}^l + \Delta T_{12}^b b - \Delta T_{12}^b a + \Delta T_{11}^h b - \Delta T_{11}^h a + \Delta A_2^{2-} \\ & + \Delta 4_1^{2+} + \Delta 4_1^{2-} b - \Delta 4_1^{2-} a + \Delta 5_1, \end{aligned}$$

which are (respectively) the number of cuspidal edge curves and the number of self-intersection closed curves.

Analogously, the variation in the number of components of the singular set and of its complement also provides nonlocal invariants; see [8].

7. Fold Maps

If we consider the particular case of fold maps (i.e., maps without cuspidal edges or swallowtail points) then the situation is simplified. Here we do not consider any strata of codimension 1 or 2 that includes a cuspidal edge. Repeating the process by which we obtain generators then yields our next theorem.

THEOREM 7.1. *Any 1-cocycle—that is, any integer-valued function I satisfying $\Delta I = 0$ on every generic homotopically trivial closed path in $C_{\text{fold}}^\infty(M, \mathbb{R}^3)$ —can be written, up to an additive constant, as a linear combination of the generators*

$$2\Delta T_{A_1 A_1^2} \quad \text{and} \quad \Delta T_{11}^{e_0} - \Delta T_{11}^{e_2} + \Delta T_{11}^{h-},$$

where $\Delta T_{A_1 A_1^2}$ denotes the sum of the increments of each of its corresponding substrata.

The first generator is a fold version of the number of triple points (here the number of triple points is equal to the Euler characteristic of the branch set, as follows from the Izumiya–Marar formula reinterpreted in this situation). The second generator is a fold version of Goryunov’s linking invariant [7] and counts the number of inverse self-tangencies in a generic regular homotopy.

However, one must note that $C_{\text{fold}}^\infty(M, \mathbb{R}^3)$ is not connected. There is no way to create a new component of the singular set once we have eliminated the 3_1 singularities because of their cuspidal edges. If we denote by $C_{\text{fold},k}^\infty(M, \mathbb{R}^3)$ the connected component of $C_{\text{fold}}^\infty(M, \mathbb{R}^3)$ where the maps have k connected components in their singular set, then the following statement results.

COROLLARY 7.2. *The first-order Vassiliev invariants for $C_{\text{fold},k}^\infty(M, \mathbb{R}^3)$ are, modulo constants, a linear combination of the number of triple points and the number of inverse self-tangencies in a generic regular homotopy from a distinguished map in the same connected component.*

8. Appendix: Bifurcation Diagrams of the Codimension-2 Strata

In this section we analyze the bifurcation diagrams of codimension-2 strata and obtain the compatibility conditions from them.

LEMMA 8.1. (a) $n_{3_1^{++}} = n_{3_1^{+-}} = n_{3_1^{--}}$; (b) $n_{4_1^{2+}} = n_{4_1^{2-}}$.

Proof. (a) Normal forms for the germs 3_2^\pm are $f(x, y, z) = (x, y, z^3 + (\pm x^2 + y^3)z)$, and a versal deformation is given by

$$F(x, y, z, u, v) = (x, y, z^3 + (\pm x^2 + y^3 + uy + v)z).$$

Analyzing the branch set $f_{u,v}(\Sigma_{f_{u,v}})$ for different values of u and v leads to the bifurcation sets shown in Figure 9. There the figures around it on the left-hand side illustrate the transitions in the branch set, the dark lines correspond to cuspidal edges, and the short lines on the codimension-1 strata mark the positive direction of the coorientation. From the bifurcation set of 3_2^+ the compatibility condition becomes $n_{3_1^{++}} = n_{3_1^{+-}}$, and from 3_2^- we obtain $n_{3_1^{+-}} = n_{3_1^{--}}$.

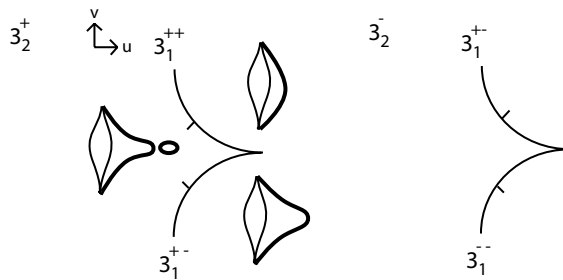


Figure 9 Bifurcation sets of 3_2^\pm

(b) The normal form of 4_1^3 is $f(x, y, z) = (x, y, z^4 + xz \pm y^3z^2)$, and a versal deformation is

$$F(x, y, z, u, v) = (x, y, z^4 + xz \pm (y^3 + uy + v)z^2).$$

The bifurcation diagram for this germ is shown in Figure 10, where the three surfaces illustrate the branch sets for different values (u, v) of the parameters outside the discriminant set. Again, the dark lines represent the cuspidal edges and the singularities are swallowtail points. This leads to the equality $n_{4_1^{2+}} = n_{4_1^{2-}}$. \square

LEMMA 8.2. $n_{A_1^2 A_2^\alpha} = n_{A_1^2 A_2^\beta} = n_{A_1^2 A_2^\gamma}$.

Proof. A versal deformation of $A_1 T_{12}$ is given by

$$\begin{cases} (x + u, y \pm x^2 + v, z^3 + yz), \\ (x, y^2, z), \\ (x^2, y, z), \end{cases} \tag{1}$$

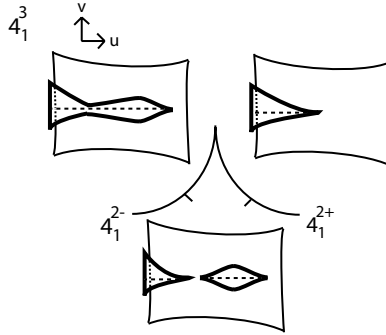


Figure 10 Bifurcation set of 4_1^3

where the + and - cases correspond (respectively) to $A_1T_{12}^b$ and $A_1T_{12}^l$. Figure 11 shows the different bifurcation diagrams. From the deformation of $A_1T_{12}^{l+}$ we obtain $n_{A_1^2A_2^\alpha} = n_{A_1^2A_2^\gamma}$, and from that of $A_1T_{12}^{b+}$ we get $n_{A_1^2A_2^\beta} = n_{A_1^2A_2^\gamma}$. Analogous results hold for $A_1T_{12}^{b-}$ and $A_1T_{12}^{l-}$. \square

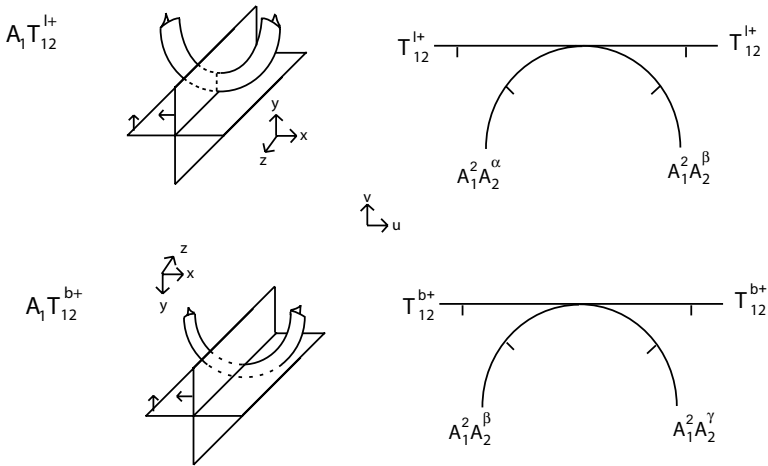


Figure 11 Bifurcation sets of $A_1T_{12}^{l+}$ and $A_1T_{12}^{b+}$

LEMMA 8.3. $n_{A_1^{4,3}} = n_{A_1^{4,4}} = 0$.

Proof. A 2-parameter deformation of $A_1^2A_3$ is given by

$$\begin{cases} (x + u, y + v, z^4 + yz + xz^2), \\ (x, y^2 + x, z), \\ (x, y^2 - x, z). \end{cases} \tag{2}$$

In Figure 12, the different possible combinations of the arrows that point in the direction of an increasing number of pre-images determine different substrata

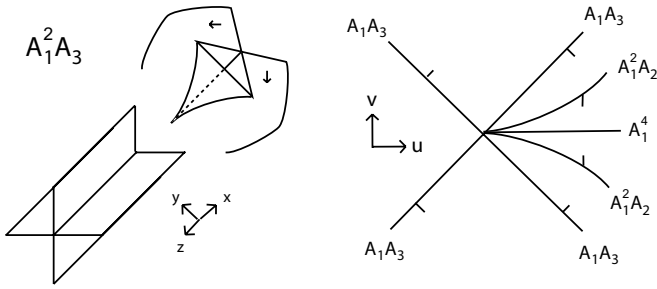


Figure 12 Bifurcation set of $A_1^2 A_3$

of codimension 1 in the bifurcation set. We observe that the presence of cusps uniquely determines the direction of the arrow in a neighborhood of the swallowtail point. It follows from Lemma 8.2 that all the substrata $A_1^2 A_2$ are equal; therefore, the two branches that appear with opposite coorientations will not contribute to the equation.

Independently of which $A_1 A_3$ substrata appear, both substrata along $u = v$ will be of the same type and so will the two along $u = -v$; these pairs of substrata will cancel out in the equation. Varying the arrows in the two planes will cause $A_1^{4,2}$, $A_1^{4,3}$, and $A_1^{4,4}$ to appear, and since all other substrata cancel out we have $n_{A_1^{4,2}} = n_{A_1^{4,3}} = n_{A_1^{4,4}} = 0$. \square

LEMMA 8.4. $n_{A_1 A_3^\alpha} = n_{A_1 A_3^\beta}$.

Proof. A versal deformation of the germ $A_1 4_1^{2-}$ is

$$\begin{cases} (x, y, z^4 + xz - (y^2 + v)z^2), \\ (x, y^2 + u, z). \end{cases} \tag{3}$$

Figure 13 shows the bifurcation set. The bifurcation set of $A_1 4_1^{2+}$ gives exactly the same equation. \square

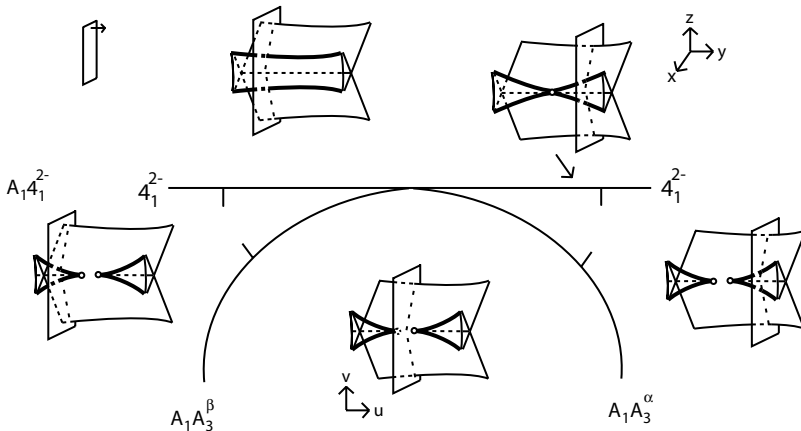


Figure 13 Bifurcation set of $A_1 4_1^{2-}$

LEMMA 8.5. $n_{A_1A_1^2}^0 = n_{A_1A_1^2}^1 = n_{A_1A_1^2}^2 = n_{A_1A_1^2}^3$.

Proof. In Figure 14 we show the bifurcation set of $DT_{A_1A_1^2}$. A versal deformation of it is

$$\begin{cases} (x, y, z^2 + x^3 + vx), \\ (x, y^2, z), \\ (x, y, z^2 + y + u). \end{cases} \tag{4}$$

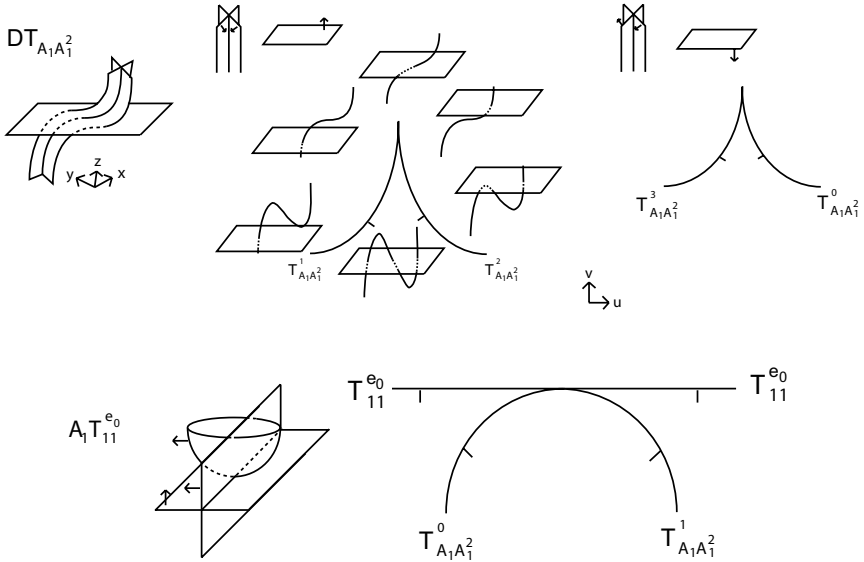


Figure 14 Bifurcation sets of $DT_{A_1A_1^2}$ and $A_1T_{11}^{e_0}$

Varying the arrows as shown in the figures, we obtain

$$n_{A_1A_1^2}^1 = n_{A_1A_1^2}^2, \quad n_{A_1A_1^2}^0 = n_{A_1A_1^2}^3.$$

A versal deformation for A_1T_{11} is

$$\begin{cases} (x + u, y + v, z^2 + x^2 + y^2), \\ (x, y, z^2), \\ (x^2, y, z). \end{cases} \tag{5}$$

We have $n_{A_1A_1^2}^0 = n_{A_1A_1^2}^1$. This, together with the other two equations, gives the desired result. □

LEMMA 8.6. $n_{T_{12}^{b-}} = n_{T_{12}^{b+}} = n_{T_{12}^{l+}} = n_{T_{12}^{l-}}$.

Proof. In Figure 15 we show the bifurcation set of DT_{12} . A versal deformation of it is

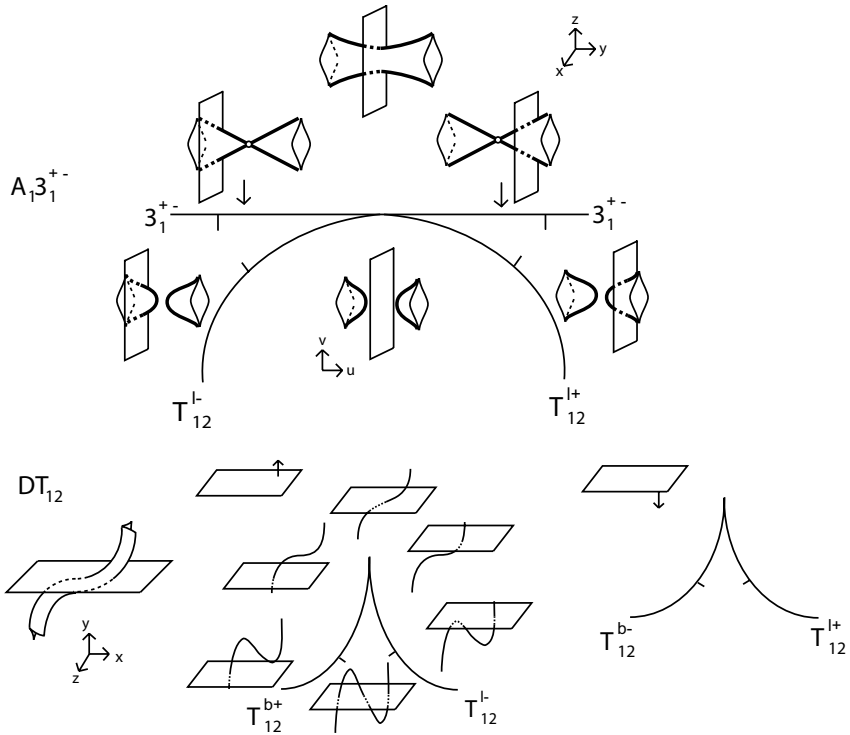


Figure 15 Bifurcation sets of DT_{12} and $A_1 3_1^{+-}$

$$\begin{cases} (x, y + x^3 + vx, z^3 + yz), \\ (x, y^2 + u, z). \end{cases} \tag{6}$$

Varying the arrow of the fold surface yields

$$n_{T_{12}^{b+}} = n_{T_{12}^{l-}}, \quad n_{T_{12}^{l+}} = n_{T_{12}^{b-}}.$$

A versal deformation of $A_1 3_1^{+-}$ is

$$\begin{cases} (x, y, z^3 + (x^2 - y^2 + v)z), \\ (x, y^2 + u, z). \end{cases} \tag{7}$$

We have $n_{T_{12}^{l-}} = n_{T_{12}^{l+}}$. This, together with the other two equations, gives the desired result. \square

LEMMA 8.7 [7]. $n_{T_{11}^{e_0}} = n_{T_{11}^{h-}} = -n_{T_{11}^{e_2}}$ and $n_{T_{11}^{e_1}} = 0$.

Figure 16 corresponds to original pictures by Goryunov in [7] adapted to our case, with modified notation. The only difference is that for Goryunov the picture

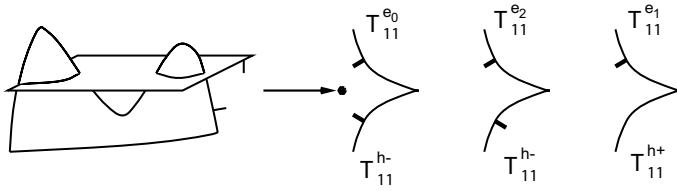


Figure 16 Bifurcation set of DT_{11}

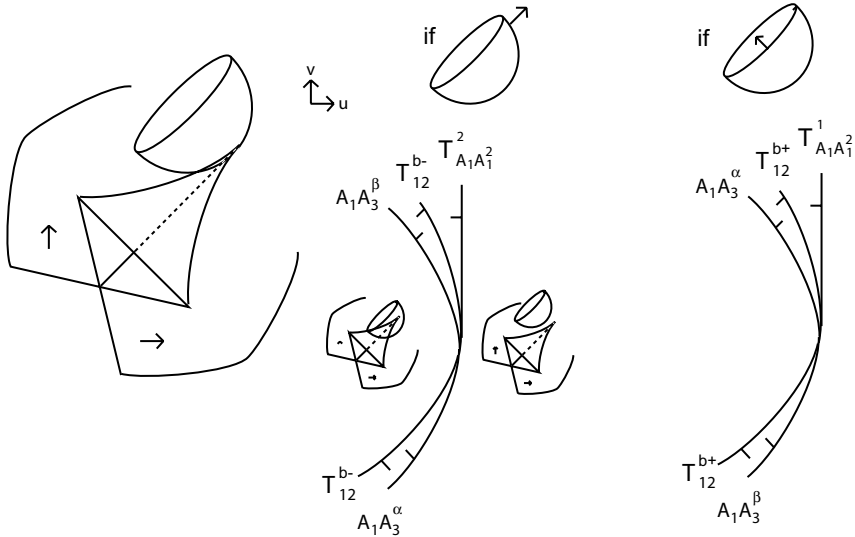


Figure 17 Bifurcation set of T_{13}

represents the image of the map whereas here it represents the branch set; however, the bifurcation diagrams are the same.

LEMMA 8.8. $n_{A_1A_3^\alpha} + n_{A_1A_3^\beta} - n_{T_{12}^{b+}} - n_{T_{A_1A_1^2}^1} - n_{T_{12}^{l+}} = 0$.

Proof. In Figure 17 we can see the bifurcation diagrams of T_{13} . Note that the tangency occurs between the fold surface and the limiting tangent vector of both the cuspidal edges and the double fold curve of the swallowtail (this is a tangency between a surface and a curve, not between two surfaces). A versal deformation is given by

$$\begin{cases} (x, y, z^4 + yz - xz^2), \\ (x + u, -x^2 - y^2 - z^2 + v, z). \end{cases} \tag{8}$$

By Lemmas 8.5 and 8.6 we have $n_{T_{A_1A_1^2}^1} = n_{T_{A_1A_1^2}^2}$, $n_{T_{12}^{b-}} = n_{T_{12}^{b+}}$, and $n_{T_{12}^{l+}} = n_{T_{12}^{l-}}$, so the equations arising from the two bifurcation diagrams are the same. \square

LEMMA 8.9. $n_{A_1A_3^\alpha} + n_{A_1A_3^\beta} - n_{A_1^2A_2^\gamma} - n_{A_2^{2-}} = 0$.

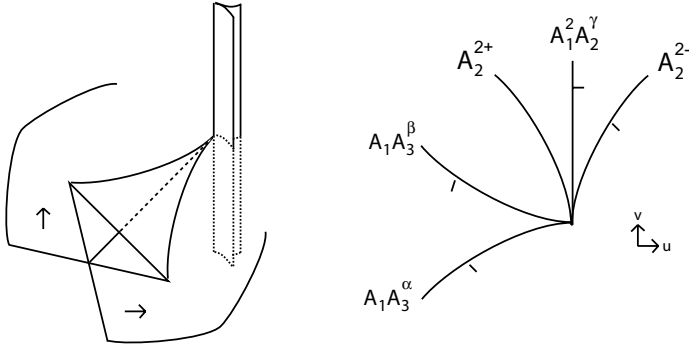


Figure 18 Bifurcation set of A_2A_3

Proof. A 2-parameter deformation of A_2A_3 is:

$$\begin{cases} (x + u, y + v, z^4 + xz + yz^2), \\ (x, y^3 + xy, z). \end{cases} \tag{9}$$

Figure 18 shows the bifurcation diagram. □

LEMMA 8.10. $n_{T_{12}^{l+}} + n_{T_{12}^{l-}} - n_{A_2^{2-}} = 0$.

Proof. Figure 19 shows the bifurcation diagram of T_{22}^1 . In the diagrams surrounding the bifurcation diagram, the line represents one of the cuspidal edges and the cusp represents a section of the other one. A versal deformation is

$$\begin{cases} (x + vz, y^3 - xy, z), \\ (x^3 - xz - y^2 + u, y, z). \end{cases} \tag{10}$$

The compatibility condition obtained is

$$n_{T_{12}^{l+}} + n_{T_{12}^{l-}} - n_{A_2^{2-}} - n_{A_2^{2+}} = 0.$$

Since A_2^{2+} is non-coorientable, the required result follows. □

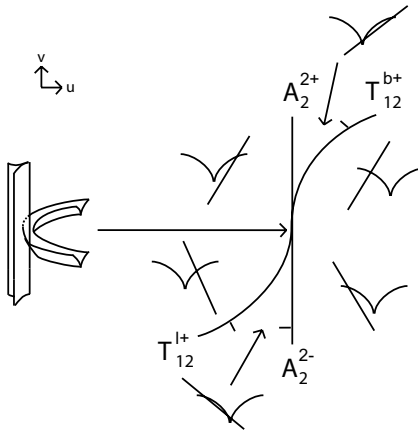


Figure 19 Bifurcation set of T_{22}^1

LEMMA 8.11. $n_{5_1} = n_{4_1^2} + n_{T_{12}}$, where 4_1^2 and T_{12} represent any of their corresponding substrata.

Proof. The normal form of 5_2 is $f(x, y, z) = (x, y, z^5 + xz + y^2z^2 + yz^3)$, and a versal deformation is

$$F(x, y, z, u, v) = (x, y, z^5 + xz + (y^2 + uy + v)z^2 + yz^3).$$

By [13] and some calculations for the multigerms strata, the bifurcation set is as shown in Figure 20; in light of Lemmas 8.1 and 8.6, we make no distinction between the different substrata of 4_1^2 and of T_{12} . The equality follows immediately. \square

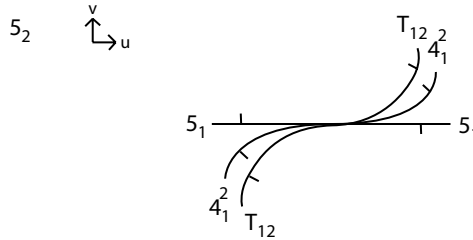


Figure 20 Bifurcation set of 5_2

LEMMA 8.12. $n_{T_{11}^{e_0}} = 0$.

Proof. Figure 21 shows the bifurcation diagram of T_{12}^1 . The cusp represents a section of the cuspidal edge and the line represents the plane. A versal deformation is

$$\begin{cases} (x^2 + vz, y, z), \\ (x^3 - xz - y^2 + u, y, z). \end{cases} \tag{11}$$

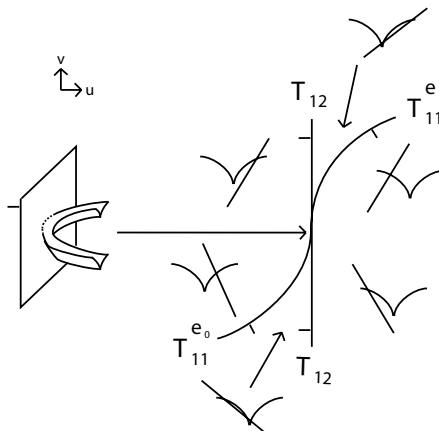


Figure 21 Bifurcation set of T_{22}^1

Given Lemma 8.6, we do not distinguish between the different substrata of T_{12} , and by Lemma 8.7 we have $n_{T_{11}}^{e_1} = 0$. The desired equation follows directly. \square

The bifurcation sets corresponding to the remaining codimension-2 strata lead to equations that are linear combinations of the equalities obtained here (possibly zero).

References

- [1] V. I. Arnold, *Topological invariants of plane curves and caustics*, Univ. Lecture Ser., 5, Amer. Math. Soc., Providence, RI, 1994.
- [2] ———, *Plane curves, their invariants, perestroikas and classifications*, Adv. Soviet Math., 21, Amer. Math. Soc., Providence, RI, 1994.
- [3] J. W. Bruce, *A classification of 1-parameter families of map germs $R^3, 0 \rightarrow R^3, 0$ with applications to condensation problems*, J. London Math. Soc. (2) 33 (1986), 375–384.
- [4] T. Cooper, D. Mond, and R. Wik Atique, *Vanishing topology of codimension 1 multi-germs over R and C* , Compositio Math. 131 (2002), 121–160.
- [5] M. Golubitsky and V. Guillemin, *Stable mappings and their singularities*, Grad. Texts in Math., 14, Springer-Verlag, New York, 1973.
- [6] V. Goryunov, *Singularities of projections of complete intersections*, J. Soviet Math. 27 (1984), 2785–2811.
- [7] ———, *Local invariants of mappings of surfaces into three space*, The Arnold–Gelfand mathematical seminars, pp. 223–225, Birkhäuser, Boston, 1997.
- [8] D. Hacon, C. Mendes de Jesus, and M. C. Romero Fuster, *Topological invariants of stable maps from a surface to the plane from a global viewpoint*, Real and complex singularities, 227–235, Lecture Notes in Pure and Appl. Math., 232, Dekker, New York, 2003.
- [9] ———, *Fold maps from the sphere to the plane*, Experiment. Math. 15 (2006), 491–497.
- [10] ———, *Stable maps from surfaces to the plane with prescribed branching data*, Topology Appl. 154 (2007), 166–175.
- [11] K. Houston, *Black and white local invariants of mappings from surfaces into three-space*, Period. Math. Hungar. 49 (2004), 49–72.
- [12] S. Izumiya and W. L. Marar, *On topologically stable singular surfaces in a 3-manifold*, J. Geom. 52 (1995), 108–119.
- [13] W. L. Marar and F. Tari, *On the geometry of simple germs of co-rank 1 maps from R^3 to R^3* , Math. Proc. Cambridge Philos. Soc. 119 (1996), 469–481.
- [14] J. A. Montaldi, *On contact between submanifolds*, Michigan Math. J. 33 (1986), 195–199.
- [15] A. M. Montesinos Amilibia, *Superficies II*, computer program available by anonymous ftp at <http://www.uv.es/~montesin/>.
- [16] T. Ohmoto and F. Aicardi, *First order local invariants of apparent contours*, Topology 45 (2006), 27–45.
- [17] R. Oset Sinha, *Topological invariants of stable maps from 3-manifolds to three-space*, Ph.D. thesis, Universitat de València, 2009.
- [18] V. Vassiliev, *Cohomology of knot spaces*, Theory of singularities and its applications, pp. 23–69, Adv. Soviet Math., 1, Amer. Math. Soc., Providence, RI, 1990.

- [19] ———, *Complements of discriminants of smooth maps: Topology and applications*, Transl. Math. Monogr., 98, Amer. Math. Soc., Providence, RI, 1992.
- [20] M. Yamamoto, *First order semi-local invariants of stable maps of 3-manifolds into the plane*, Proc. London Math. Soc. (3) 92 (2006), 471–504.

R. Oset Sinha
Facultad de Matemáticas
Departamento Geometría y Topología
Universitat de València
46100 Burjasot
Valencia
Spain
raul.osest@uv.es

M. C. Romero Fuster
Facultad de Matemáticas
Departamento Geometría y Topología
Universitat de València
46100 Burjasot
Valencia
Spain
carmen.romero@uv.es